World Journal of Biology Pharmacy and Health Sciences
eISSN: 2582-5542
Cross Ref DOI: 10.30574/wjbphs
Journal homepage: https://wjbphs.com/

(RESEARCH ARTICLE)

Check for updates

Quality by design approach for development and optimization of rifampicin loaded nanoparticles and characterization

Amaravathi Vyshanavi [1,*], N. Pradeep kumar [1], C. Manjula [1] and A. Srikanth [2]

[1] *Department of Pharmaceutics, Vasavi Institute of pharmaceutical sciences, Peddapalli(v) Near, Bhakarapeta railway station, Siddavatam(M), Kadapa, A.P India.*
[2] *Department of pharmaceutical analysis, Vasavi Institute of pharmaceutical sciences, Peddapalli(v) Near, Bhakarapeta railway station, Siddavatam(M), Kadapa, A.P India.*

World Journal of Biology Pharmacy and Health Sciences, 2023, 20(03), 124–137

Publication history: Received on 24 September 2023; revised on 14 November 2023; accepted on 16 November 2023

Article DOI: https://doi.org/10.30574/wjbphs.2023.16.3.0468

Abstract

Background: Rifampicin is an effective in the treatment of sensitive, non-resistant strains of mycobacterium tuberculosis. Thus there is need to develop a rifampicin loaded nanoparticles.

Aim: This study is focused on development of RFM loaded nanoparticles, characterization to achieve lung targeting using quality by design approach.

Objectives: The main objective of this study is optimizing particle size and entrapment efficiency of rifampicin-loaded nanoparticles and making them suitable for nebulizer application using QbD approach.

Methods: Quality target product profile was defined along with critical quality attributes for the formulation. Preparation of nanoparticle dry powder inhaler formulation were numerous methods such as microemulsion solvent evaporation, ionic gelation and modified ionic gelation followed by probe sonication were employed for the preparation of nanoparticles and the final method of preparation was selected based on particle size, zeta potential, entrapment efficiency and drug loading.

Results: The optimized RFM-loaded nanoparticles were characterized by UV spectroscopy, FTIR, DSC techniques. The observed nanoparticles were spherical in shape. The TPP concentration, stirring speed and concentration of acetic acid were playing a crucial role in the successful formation of nanoparticles and were selected for optimization. In vitro release study showed 100% release of pure RFM within 12 hrs and the optimized chitosan nanoparticle formulation loaded with RFM showed nearly 90% release of RFM within 24 hr.

Conclusion: Rifampicin loaded nanoparticle DPI formulations achieve lung targeting and the delivery of drug into the lungs will also prevent the first pass metabolism, thus, leading to reduction in the dose of the drug as well as related side effects. These drug targeting approaches may serve as a boon in the effective treatment of tuberculosis.

Keywords: Concentration; Drug; Nanoparticle; Rifampicin; Release; Qbd.

* Corresponding author: Amaravathi Vyshanavi

1. Introduction

Tuberculosis (TB) is one of the deadliest diseases amongst the infectious diseases, despite the use of several antibiotics and live attenuated vaccines. So, it becomes essential to study the genetics and physiology of mycobacterium tuberculosis [1]. The mycobacterium tuberculosis has been originated from soil and that some species progressed to live in mammals. Prior to AIDS epidemic, one study showed that 85% of new cases are that of pulmonary TB. Mycobacterium tuberculosis flourishes through various stages [2]. WHO in 1970 recommended a drug regime consisting of four first line drugs- isoniazid (INH), rifampicin (RFM), pyrazinamide (PZN) and ethambutol (ETB) [3]. This regime can be used for the effective treatment of sensitive, non-resistant strains of Mycobacterium tuberculosis [4]. The patient has to face severe side effects such as nausea and hepatotoxicity. For this reason, the patients do not remain stick to the regime. Owing to the limitations of the current treatment regime, the researchers are working for the development of newer drugs (effective against both non-resistant and resistant bacteria) as well as novel drug delivery systems for efficient targeting [5]. Pulmonary drug delivery systems have numerous challenges. One of the major challenges is the enzymatic degradation of the inhaled drugs by cytochrome P-450 iso-forms present in the lungs [6]. The delivery of proteins and peptides is also a significant challenge due to the presence of protease and peptidase enzymes [7]. The bioavailability of drug also poses a major challenge as it is dependent on the technique of inhalation as well as the size of the inhaled particles. The size of the drug particles to settle deep into the lungs must be in the range of 1-5 μm. The delivery of such small particle size into the lungs requires a significantly optimized formulation [8]. The most common aerosol formulations for pulmonary drug delivery are: Nebulizers, metered dose inhalers (MDIs) and dry powder inhalers (DPIs) [9]. Chitosan is a natural polymer is an apt choice for pulmonary drug delivery because of its low toxicity, good anti-microbial and anti-bacterial properties. Chitosan is gaining a lot of attention for the delivery of genes, drugs and vaccines due to its biodegradable nature [10]. The Selected drug for current studies due to their lipophilic nature which may lead to their greater retention in the lungs [11]. Considering the dose and the side effects of RFM, several studies have been reported presenting RFM in different formulation strategies. Taking into consideration the limitations associated with such high oral doses of drugs, we have prepared DPI formulations of both the drugs in order to achieve lung targeting. The delivery of drug into the lungs will also prevent the first pass metabolism, thus, leading to reduction in the dose of the drug as well as related side effects. These drug targeting approaches may serve as a boon in the effective treatment of tuberculosis.

2. Materials and method

Rifampicin (RFM), Hydroxy propyl methyl cellulose capsules was obtained from Cipla Ltd. Mumbai, India. Lactose α-monohydrate from Meggle Germany, Chitosan from Esvee Agro and Feeds, Pune, India, Sodium tri polyphosphate from Sigma Aldrich USA, and Tween-80, Acetic acid obtained from CDH Chemicals, Mumbai, India.

2.1. Methodology

2.1.1. Preparation standard stock solution

The standard stock solution was prepared in water: acetonitrile in the ratio 55:45. An accurately weighed 100 mg of RFM was dissolved in freshly prepared 100 mL water: acetonitrile. From this solution, 10 mL was taken and further diluted to 100 mL with water: acetonitrile to yield the standard stock solution (100μg/mL).

2.1.2. Preparation of buffer pH 2.27

The buffer of pH 2.27 was prepared by adjusting the pH of distilled water to 2.27 with o- phosphoric acid.

2.1.3. Differential scanning calorimetry [12]

The differential scanning calorimetry (DSC) studies of free RFM was analyzed using thermal analyzer. The sample was heated after hermetically sealing in an aluminium pan at 10°C/min of heating rate in temperature range of 50-300°C under nitrogen atmosphere purged at a flow rate of 20 mL/min.

2.1.4. Saturation solubility studies of rifampicin in different buffers

Excess amount of RFM was added to different solvents (0.1 N HCl, phosphate buffer pH 6.8 and 7.4) in stoppered vial. The vials were allowed to shake on rotary shaker for 24 hrs. After 24 hrs, the drug concentration in different solvents was determined using UV spectrophotometer.

2.1.5. Drug excipient compatibility studies [13]

The drug and carrier remain in intimate contact with each other due to thorough mixing in DPI formulations as well as in nanoparticle formulations. Hence, compatibility studies are necessary to be done. The drug excipient compatibility studies were done using Fourier transform infrared (FTIR) spectroscopy. The powder blend of drug and excipients were mixed with KBr in 1:1 ratio and FTIR spectra were recorded in the range of 4000-400 cm-1 after storage of 1 month.

2.1.6. Formulation development

Micronized drug was taken in a vial and lactose was added to drug in various ratios. Further, both drug and lactose were mixed with the help of a vortex mixer. The dry powder was filled in a capsule and was evaluated for various parameters.

2.2. Preparation of nanoparticle dry powder inhaler formulation

2.2.1. Method selection

Numerous methods such as microemulsion solvent evaporation, ionic gelation and modified ionic gelation followed by probe sonication were employed for the preparation of nanoparticles and the final method of preparation was selected based on particle size, zeta potential, entrapment efficiency and drug loading[14].

2.2.2. Microemulsion solvent evaporation method

Chitosan was dissolved in acetic acid with continuous stirring. RFM was dissolved in dichloromethane. The drug solution was added dropwise in chitosan solution with continuous stirring for 2 hrs at 60°C. The above solution was further added in tween-80 solution with continuous stirring at 1500 RPM for 24 hrs to ensure complete evaporation of dichloromethane.

2.2.3. Ionic gelation method

Chitosan was dissolved in acetic acid at 1000 RPM. Tween-80 solution was added in the above solution. RFM was dissolved in sodium tri poly phosphate (TPP) solution. The drug solution was added dropwise in chitosan solution with continuous stirring for 45 mins at 1200 RPM.

2.3. Modified ionic gelation and probe sonication method

Chitosan was dissolved in acetic acid at 600 RPM on magnetic stirrer. Thereafter, 5 mL of Tween-80 solution was added to the chitosan solution. RFM was dissolved in the prepared solution. TPP was added dropwise in the drug solution after filtration through 0.45 µ syringe filter. This solution was then allowed to stir for 24 hrs and probe sonicated for 2 mins.

2.3.1. Effect of various parameters on the preliminary batches

Effect of various parameters affecting the formulation such as amount of polymer and chitosan/TPP ratio, acetic acid concentration, tween 80 concentration and stirring speed were studied on entrapment efficiency and drug loading to optimize the formulation.

2.3.2. Effect of polymer amount and chitosan/TPP ratio

The batches with polymer amounts of 200, 300, 400 and 500 mg were evaluated and chitosan/TPP ratio of 3:0.5, 3:1 and 3:2 were evaluated for entrapment efficiency and drug loading (Batches C1P to C4P and batches C1S to C3S).

2.3.3. Effect of acetic acid concentration

The batches with acetic acid concentrations of 0.5,1,2,3 and 4% were evaluated for entrapment efficiency and drug loading (Batches C1A to C5A).

2.3.4. Effect of tween 80 concentration

The batches were evaluated for entrapment efficiency and drug loading with various tween 80 concentrations such 0.5,1 and 2% (Batches C1T to C3T).

2.3.5. Effect of stirring speed

The batches were evaluated for entrapment efficiency and drug loading at stirring speeds of 600, 1200 and 1800 rpm (Batches C1R to C3R).

However, in BDQ nanoparticle formulation the significant factors were screened using Plackett-Burman design. The parameters screened were polymer amount, TPP concentration, acetic acid concentration, tween 80 concentration, stirring speed, temperature and probe sonication time.

2.3.6. Optimization of the nanoparticle formulation

The optimization of the RFM nanoparticle formulation was carried out using Box Behnken design. The TPP concentration, acetic acid concentration and stirring speed were taken as the independent variables and 15 batches were prepared as per the design. The BDQ nanoparticles were optimized using 23 factorial design using polymer amount (X1), TPP concentration (X2) and probe sonication time (X3) as the independent variables. The particle size, zeta potential, entrapment efficiency and drug loading were taken as the response parameters.

2.4. Evaluation parameters for the nanoparticle formulation [15]

2.4.1. Particle size and zeta potential

The particle size was determined by Malvern Mastersizer (Pai et al; 179–195). The nanoparticles were suspended in methanol containing 0.1% tween 80 to prevent nanoparticle aggregation and average particle size was determined. For the zeta potential measurements, the particles were suspended in de-ionized water.

2.4.2. Entrapment efficiency and drug loading

The nanoparticles were separated after centrifugation at 19,000 rpm for 30 mins. For the preliminary batches of RFM, the supernatant was analyzed using UV spectroscopy with phosphate buffer pH 7.4 as the solvent. For the optimization batches, the supernatant was analyzed using buffer pH 2.27: acetonitrile (55:45) as the mobile phase for RFM.

$$Entrapment\ efficiency = \frac{Total\ amount\ of\ drug - Amount\ of\ drug\ in\ supernatant}{Total\ amount\ of\ drug} * 100 \text{..Equation 4.6}$$

$$Drug\ loading = \frac{Total\ amount\ of\ drug - Amount\ of\ drug\ in\ supernatant}{Amount\ of\ polymer} * 100 \text{.....Equation 4.7}$$

2.4.3. Scanning electron microscopy

The surface morphological studies of pure drug and drug loaded nanoparticles were carried out using scanning electron microscope (SEM). The method used was plasma deposition method which employed a gold coating unit to fabricate the sample surface conductive to electron beam. The gold coating was done under argon atmosphere at 40-100°A.

2.4.4. In vitro drug release [16]

In vitro drug release studies were carried out using dialysis bags that allow free diffusion of drug into the release medium. The drug release studies were done with phosphate buffer pH 7.4 as the release medium. Exactly, 50 mg free RFM and nanoparticle formulation equivalent to 50 mg RFM (5 mg in case of BDQ) were placed in the dialysis bags. The bags were tied at both the ends and placed in the release medium. The release studies were carried out at predetermined intervals (2, 4, 6, 8, 10, 12, 16, 18 and 24 hrs). At all the points, 1mL of sample was taken and replaced with fresh medium. The withdrawn samples were then analyzed using HPLC. In BDQ studies, 5 mg of free BDQ and nanoparticle formulation equivalent to 5 mg BDQ were taken for the in vitro release medium (based on the dose calculation of the drugs).

3. Results and discussion

3.1. Determination of UV absorption maxima of rifampicin in different buffers

In the present study, the U.V spectrophotometry was used for estimation of RFM. The absorption maxima were determined in phosphate buffer pH 7.4, phosphate buffer pH 6.8 and 0.1N HCl. The absorption maxima of RFM were observed at 475 nm. The results are shown in Figure 1a-1c.

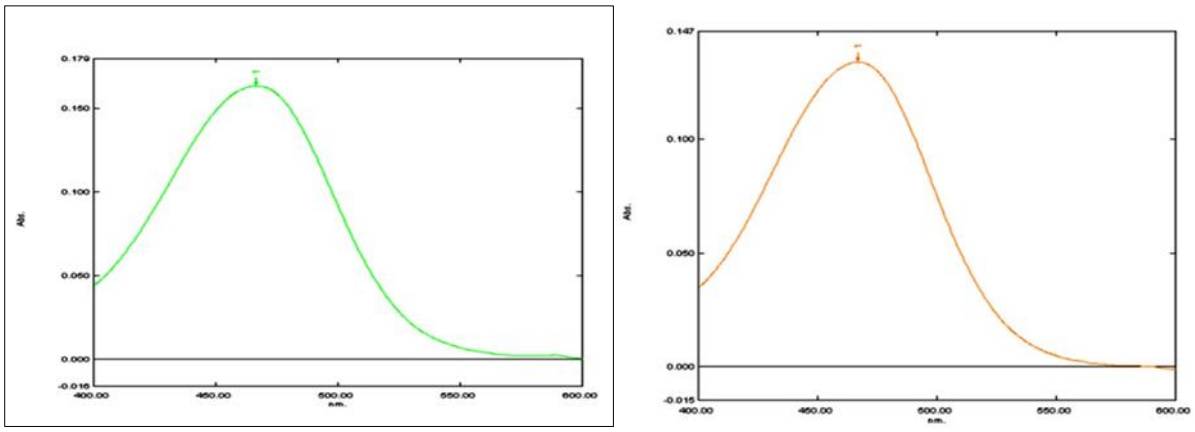

Figure 1a-1c UV absorption maxima of RFM in phosphate buffer pH 7.4, pH 6.8 and 0.1 N hydrochloric acid

3.1.1. Preparation of standard curve

From the stock solution (100 µg/mL), 10, 25, 40, 50, 60 and 75 mL was taken and diluted upto 100 mL with water: acetonitrile (55:45). The peak area for different dilutions was determined at 230 nm using buffer pH 2.27: acetonitrile (55:45) as the mobile phase. The results and standard curves are shown in Table 1 and Figure 2.

Table 1 Results of HPLC analysis of rifampicin in water: acetonitrile (55:45) with buffer pH 2.27: acetonitrile (55:45) as the mobile phase

Concentration (µg/mL)	Peak area (mAU*s)(Mean of three values ± SD)
10	133.08 ± 0.01
25	328.60 ± 0.11
40	535.32 ± 0.53
50	666.52 ± 0.57
60	789.95 ± 0.26
75	988.10 ± 0.06

The linearity of RFM was found within the concentration range of 10-75 µg/mL.

3.1.2. Differential scanning calorimetry

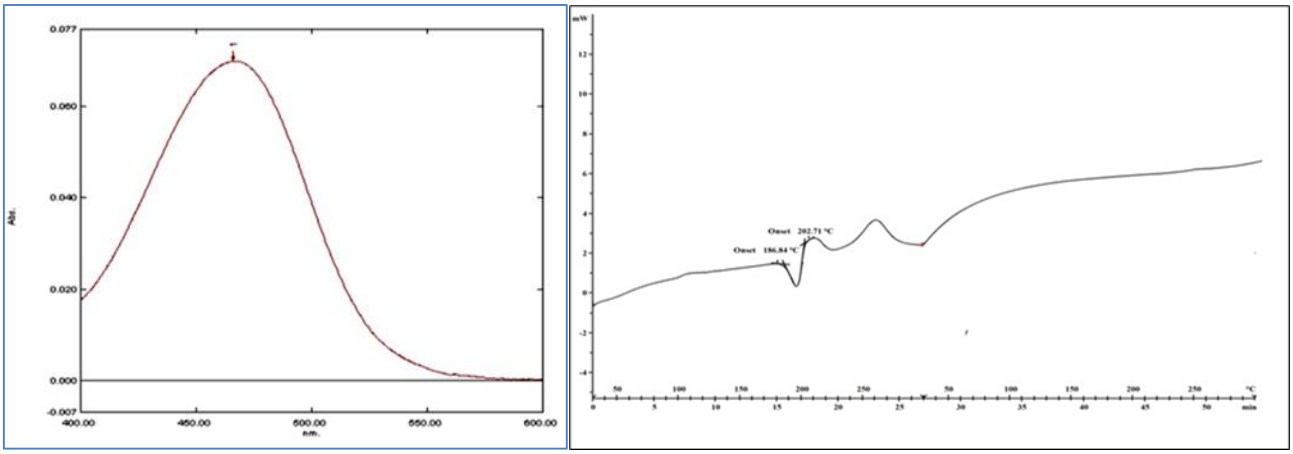

Figure 2 Differential scanning calorimetry of rifampicin

The corresponding melting point peak of rifampicin at 186.84°C confirms its identification. The results are shown in figure no.2.

Table 2 Solubility profile of rifampicin in different buffers

Solvents	Solubility (mg/mL) for RFM	Solubility profile
0.1 N HCl	180	+++++
Phosphate Buffer pH 6.8	9.9	+++
Phosphate Buffer pH 7.4	10.8	+++

*+ = very slightly soluble, ++=slightly soluble, +++= soluble, ++++ =freely soluble, +++++= very soluble

3.2. Compatibility studies of rifampicin

The peaks and the functional groups of RFM are illustrated in Table no. 3 which were also present in the mixture of RFM with the lactose as can be seen in the overlay spectra of RFM and its mixture with lactose. The peaks were also present in the mixture of RFM with chitosan and TPP as shown in Figure 3.

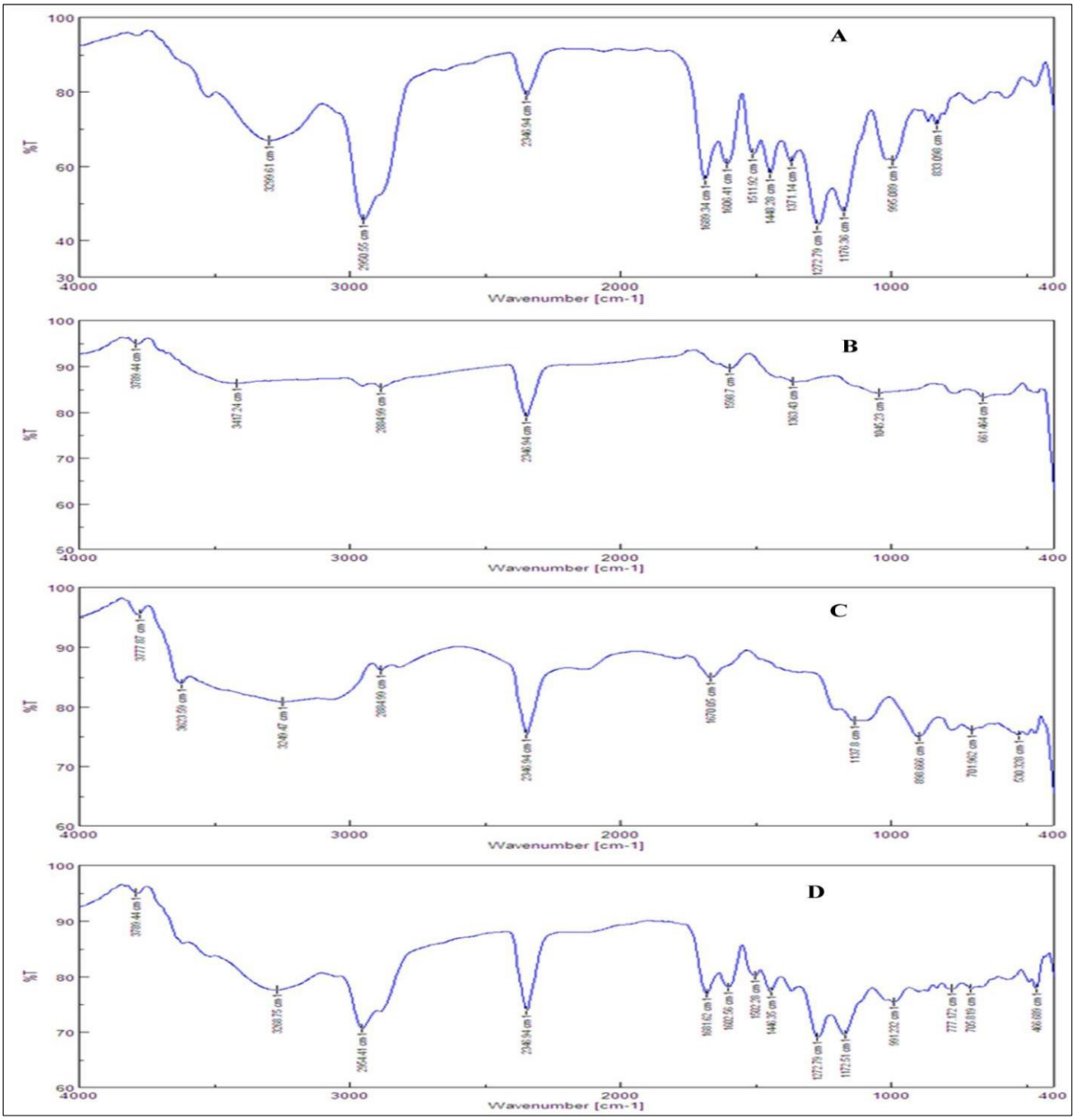

Figure 3 FTIR of (a) pure RFM, (b) chitosan, (c) TPP, and (d) mixture of RFM with all the excipients.

Table 3 Functional groups corresponding to FTIR peaks of rifampicin

Wavenumbers (cm^{-1})	Functional Groups
3299.61	-OH
2954.41	-CH aliphatic
1689.34	-C=O
1606.41	-CN

3.3. Preliminary studies

3.3.1. Method selection

The positive zeta-potential values indicate that the surface of the nanosystems is mostly composed of chitosan. This net positive charge of the particle is desirable to promote electrostatic interaction with the negatively charged sialic acid on the alveolar macrophages. Depending upon the above results of entrapment efficiency and drug loading, further batches were prepared with modified ionic gelation- probe sonication method.

Table 4 Method selection for the preparation of nanoparticles

Method	Particle size (nm)	Zeta potential (mV)	Entrapment efficiency (%)	Drug loading (%)
A (Microemulsion solvent evaporation)	627.0 ± 4.1	57.1 ± 1.2	16.5±1.9	2.0± 0.3
B (Ionic gelation)	580.9 ± 3.2	56.4 ± 4.4	35.7± 2.1	4.5± 0.5
C (Modified ionic gelation and probe sonication)	409.6 ± 1.8	55.5 ± 0.7	46.8± 0.3	5.8±0.1

3.4. Effect of polymer amount and chitosan/TPP ratio

The lower value of entrapment efficiency and drug loading in Batch C1P can be attributed to the fact that less number of nanoparticles were formed due to less concentration of chitosan. An increase in chitosan (Batch C4P) also led to decreased drug loading and entrapment efficiency. This may be explained by the fact that relatively higher viscosity of the higher chitosan concentration hinders the drug encapsulation.

Table 5 Study of effect of different polymer amounts on the nanoparticle preparation

Batches	Amount of polymer (mg)	Entrapment efficiency (%)	Drug loading (%)
C1P	200	25.2 ±2.1	6.7 ± 0.4
C2P	300	47.6 ± 1.3	7.9 ± 0.06
C3P	400	46.8 ±0.6	5.8 ± 0.02
C4P	500	37.1 ±3.4	3.7 ± 0.10

* Amount of RFM= 50 mg; TPP=0.1%; acetic acid=2%

3.5. Effect of different chitosan/TPP ratios on the nanoparticle preparation

At CS/TPP ratio of 3:0.5, drug loading and entrapment efficiency were found to be less. This might be due to the fact that proper matrix might not have been found which may have led to less drug loading and entrapment efficiency. The encapsulation efficiency and loading capacity of nanoparticles decreased with the decrease in weight ratio of chitosan/TPP of 3:2. A possible explanation for this may be due to the increase in TPP, the aggregation of nanoparticles occur which indicate the reduction of encapsulation efficiency.

Table 6 Study of effect of different chitosan/TPP ratios on the nanoparticle preparation

Batches	CS/TPP	Entrapment efficiency (%)	Drug loading (%)
C1S	3:0.5	44.2 ± 3.1	7.37 ± 3.2
C2S	3: 1	69.1 ± 0.4	11.5 ± 0.9
C3S	3: 2	46.3 ± 2.4	7.7 ± 2.2

*CS= Chitosan; TPP= Sodium tri poly phosphate

3.5.1. Effect of concentration of acetic acid

On increasing the concentration of acetic acid, entrapment efficiency and drug loading increased. This might be due to easier solution of chitosan and a better dispersion of chitosan particles. Not much difference was seen in the entrapment efficiency after increasing the concentration of acetic acid after 2%. Hence the concentration showing the highest value of entrapment efficiency and drug loading was taken in the optimization design.

Table 7 Study of effect of concentration of acetic acid on the nanoparticle preparation

Batches	Concentration of acetic acid (%)	Entrapment efficiency (%)	Drug loading (%)
C1A	0.5	26.9 ± 0.7	4.5 ± 0.5
C2A	1	47.6 ± 1.3	7.9 ± 0.1
C3A	2	69.1 ± 0.9	11.5 ± 0.2
C4A	3	66.1 ± 2.7	10.0 ± 0.9
C5A	4	63.9 ± 4.3	9.3 ± 0.1

*Amount of RFM=50 mg; chitosan= 300 mg; TPP=0.1%

3.5.2. Effect of tween-80 concentration

On varying the concentration of Tween-80, not much difference was found in the entrapment efficiency and drug loading. Hence, the tween-80 concentration of 1% was used in all the batches.

Table 8 Study of effect of different tween-80 concentrations on nanoparticle preparation

Batches	Tween- 80 concentration (%)	Entrapment efficiency (%)	Drug loading (%)
C1T	0.5	65.6 ± 4.1	10.5 ± 0.9
C2T	1	69.1 ± 2.2	11.5 ± 0.9
C3T	2	67.4 ± 1.3	11.1 ± 0.3

*Amount of RFM=50 mg; chitosan=300 mg; TPP=0.1%; acetic acid=2%

3.6. Effect of stirring speed on the nanoparticle preparation

Table 9 Study of effect of different stirring speeds on the nanoparticle preparation

Batches	Stirring speed (RPM)	Entrapment efficiency (%)	Drug loading (%)
C1R	600	38.9± 2.1	6.5 ± 0.3
C2R	1200	69.1±2.2	11.5 ± 0.9
C3R	1800	67.1±2.4	10.4 ±1.6

*Amount of RFM=50 mg; chitosan=300 mg; TPP=0.1%; acetic acid=2%; tween-80=1%

On increasing the stirring speed from 600 rpm to 1200 rpm, entrapment efficiency and drug loading increased from 38.90 to 69.12% and 6.5% to 11.5% respectively. But further not much effect was found on entrapment efficiency and

drug loading at 1800 rpm. Hence the speed showing highest entrapment efficiency and drug loading was considered in the optimization design.

3.6.1. Optimization of the formulation using Box-Behnken design

The response surface designs refer to a combination of statistical procedures employed to study the effects of several independent variables on the formulation development. Box behnken design consists of fewer design points are cost effective. Therefore, 3- factor 3-level box behnken design was used to optimize nanoparticle formulation to achieve optimum response. The objective of the optimization design was to get optimum particle size and maximize entrapment efficiency and drug loading. The desired particle size for drug localization in alveoli upon administration via inhalation should be within the range of 50-200 nm. Hence, this range was targeted for particle size and maximum amount of drug entrapment and drug loading were set as criteria for optimization. The preliminary studies suggested the relevance of three variables including, concentration of TPP and acetic acid and stirring speed. Eventually, box-behnken design was applied for the optimization of the formulation by taking concentration of TPP (X1), concentration of acetic acid (X2) and stirring speed (X3) as independent variables. Fifteen batches were prepared and evaluated for various parameters (Table 10).

Table 10 Transformed values of design batches

Batches	TPP Concentration (X1)	Conc. of acetic acid (X2)	Stirring speed (X3)
C1	-1	-1	0
C2	+1	-1	0
C3	-1	+1	0
C4	+1	+1	0
C5	-1	0	-1
C6	+1	0	-1
C7	-1	0	+1
C8	+1	0	+1
C9	0	-1	-1
C10	0	+1	-1
C11	0	-1	+1
C12	0	+1	+1
C13	0	0	0
C14	0	0	0
C15	0	0	0

TPP concentration: -1, 0 and +1 represents 0.05%, 0.10% and 0.15%; **Acetic acid concentration:** -1, 0 and +1 represents 0.5%, 2.0% and 3.5%; **Stirring speed:** -1, 0 and +1 represents 800 rpm, 1200 rpm and1600 rpm

The preliminary trials were done to understand the effect of various variables on product quality. The nanoparticles were prepared using ionic gelation and probe sonication method. It was observed that increase in amount of chitosan from 300 mg to 500 mg resulted into decrease in drug entrapment. This may be due to increase in viscosity of solution. The tween-80 concentration did not show much effect on the entrapment efficiency and drug loading. Hence, the chitosan amount and tween-80 concentration were fixed at 300 mg and 1% based on the preliminary trials. However, an increased TPP concentration showed the gelling due to the aggregation of the nanoparticles. The stirring speed and concentration of acetic acid also showed high impact on drug entrapment inside the nanoparticles as well as drug loading. Hence, the TPP concentration, stirring speed and concentration of acetic acid were playing a crucial role in the successful formation of nanoparticles and were selected for optimization.

3.7. Characterization of the nanoparticles

3.7.1. Effect of variables on particle size

The particle size analysis was seen as one of the important parameters for the formulation of nanoparticles. The developed particles were found within the range of 124.1 ± 0.2 nm to 402.3 ± 2.8 nm. The positive effect left by the acetic acid concentration on size of nanoparticles was attributed to better solubility and dispersion of chitosan nanoparticles. The increase in stirring speed showed a negative effect on the size of nanoparticles. The decrease in particle size from 402.3 nm to 124.1 nm was seen when stirring speed was increased from 800 rpm to 1200 rpm. This decrease in particle size was estimated because of increased mechanical shear at greater stirring speed. However, only the acetic acid concentration showed the significant effect ($p=0.0325$) on particle size in comparison to TPP concentration and stirring speed ($p>0.05$).

Polydispersity index (PDI) was observed in the range of 0.195-0.594 in the design batches. The positive zeta potential was due to the presence of positively charged chitosan in the formulation. The net positive charge of nanoparticles is indeed an inevitable requirement to promote electrostatic interaction with negatively charged sialic acid present on the surface of alveolar macrophages, which helps achieving greater uptake of RFM-loaded nanoparticles by alveolar macrophages.

3.7.2. Effect of variables on percent entrapment efficiency

The increased TPP concentration may have led to higher cross linking which, in turn, hindered the sizeable encapsulation of RFM in nanoparticles. Further, increased acetic acid concentration drove the increase in entrapment efficiency from 32.61± 1.7 % to 71.94 ± 0.1%. This increase was due to the complete solubility of chitosan in 1% acetic acid. Also, increase in the stirring speed from 800 rpm to 1200 rpm also led to the increase in % entrapment efficiency. This sizeable increase in entrapment efficiency was seen due to the formation of compact nanoparticles because of greater shear.

3.7.3. Effect of variables on percent drug loading

The negative effect rendered by an increase in TPP concentration on % drug loading whereas the acetic acid concentration and stirring speed showed an increase in % drug loading. The concentration of TPP and acetic acid showed the significant effect on both entrapment efficiency ($p=0.0445$ and 0.0022) and drug loading ($p=0.0416$ and 0.0026) in comparison to stirring speed ($p>0.05$). Hence, it was observed that stirring speed was showing the least impact on all the responses as compared to TPP concentration and acetic acid concentration. Thus, design expert generated contour plots for concentration of TPP and acetic acid keeping the stirring speed constant at 1200 rpm.

The contour plots of particle size, % entrapment efficiency, % drug loading, and overlay plot are shown in Fig. The batches (C13, C14 & C15) with the same composition showed reproducible results with the smallest particle size (Fig. 4) and greater entrapment efficiency.

Table 11 Composition of the optimized nanoparticle batch of RFM

Optimized batch	Amount of drug (mg)	Amount of chitosan (mg)	Concentration of TPP (%)
C15	50	300	0.1

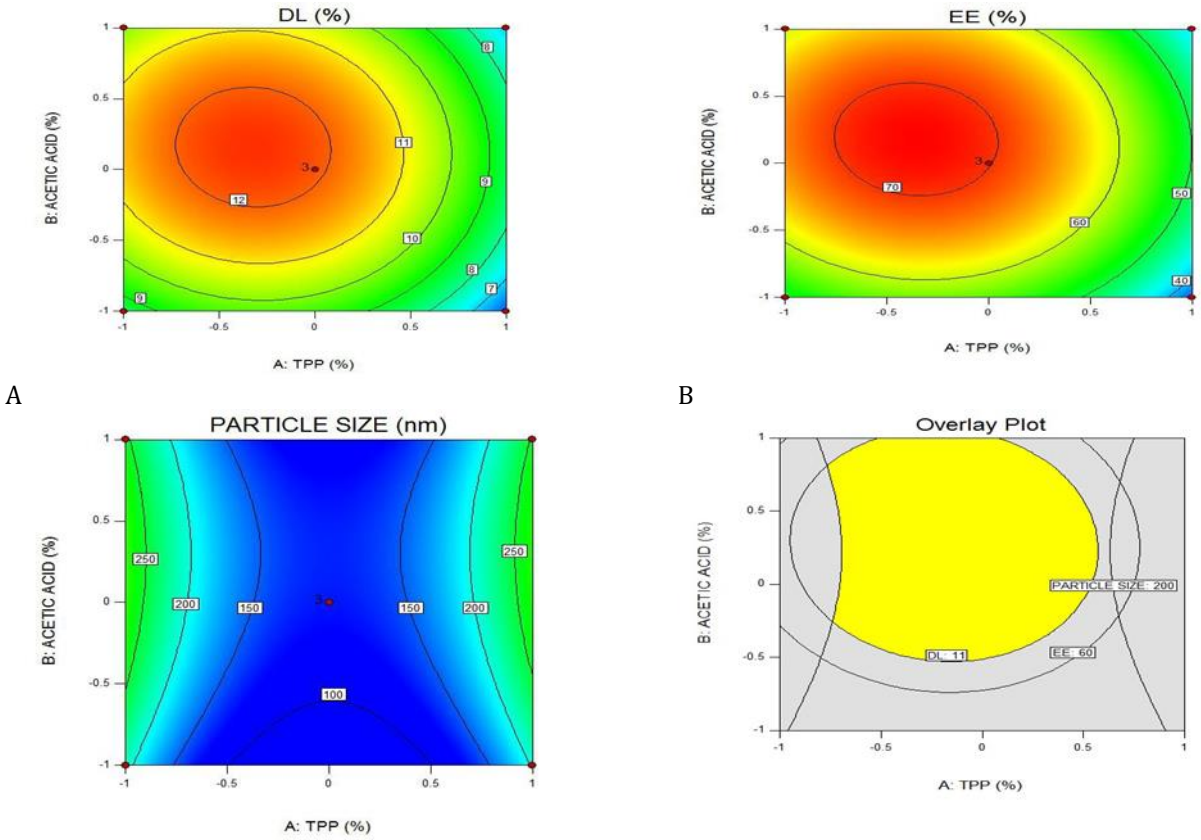

Figure 4 Contour plots corresponding to A. Entrapment efficiency, B. Drug loading, C. Particle size and D. Overlay plot showing design space.

The optimized nanoparticle batch of RFM as suggested by Design Expert 7.0.0 software has the following composition.

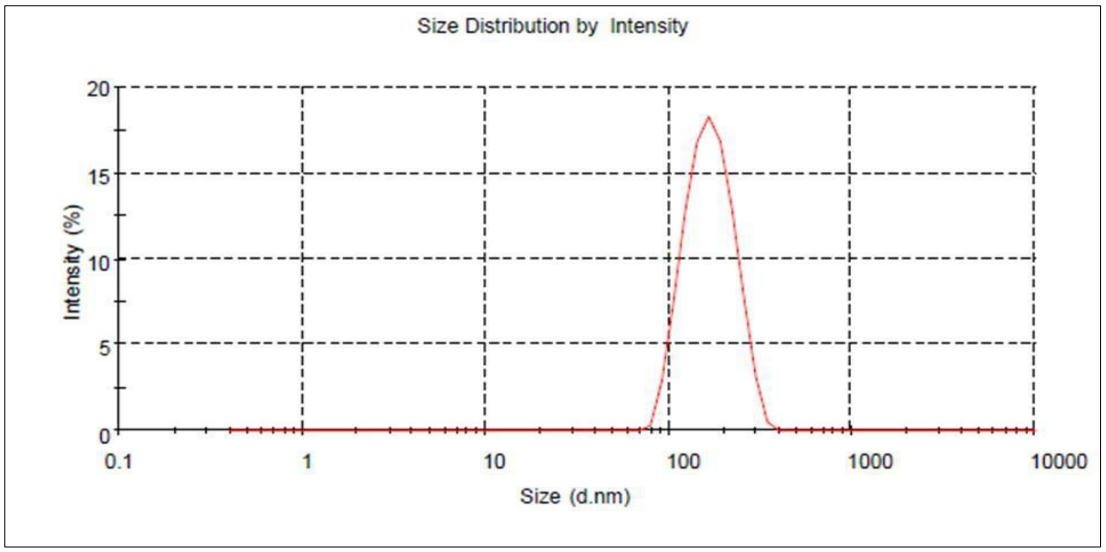

Figure 5 Particle size of the optimized batch C15

Table 12 Characterization of RFM nanoparticles with respect to particle size, polydispersity index, Zeta potential, % entrapment efficiency, and % drug loading

Batch code	Particle size (nm)	PDI	Zeta potential (mV)	EE (%)	DL (%)
C1	170.1 ± 0.4	0.333 ± 0.01	57.1 ± 0.5	52.44± 0.5	8.74± 0.3
C2	172.4 ± 0.4	0.191 ± 0.01	56.4±1.3	37.59± 0.5	6.27± 0.1
C3	286.5 ± 1.1	0.226 ± 0.05	55.5±1.5	58.87± 1.1	9.81± 1.9
C4	293.1 ± 1.6	0.141 ± 0.02	54.9±1.1	39.57± 1.5	6.59± 1.6
C5	281.6 ± 1.7	0.594 ±0.15	52.1±0.9	56.79 ± 2.3	9.47± 2.0
C6	311.2 ± 1.2	0.208 ± 0.09	56.2±0.1	55.10 ± 1.5	9.18± 1.5
C7	402.3 ± 2.0	0.313 ± 0.08	55.9±0.6	63.67± 3.1	10.61± 2.8
C8	346.9 ±1.5	0.189 ± 0.04	51.5±0.9	32.61± 1.7	5.44 ± 1.6
C9	172.5 ± 0.8	0.246 ± 0.07	50.6±1.1	45.28± 0.9	7.55± 1.1
C10	127.8 ± 0.2	0.401 ± 0.15	49.5±1.2	66.22± 0.1	11.04± 0.3
C11	153.9 ± 0.3	0.303 ± 0.07	51.1±0.2	51.16± 0.4	8.53± 0.4
C12	155.7 ± 0.4	0.289 ± 0.04	50.8±0.1	49.76± 0.5	8.29± 0.5
C13	136.2 ± 0.5	0.291 ± 0.03	59.1 ±0.2	67.93± 0.3	11.44± 0.6
C14	129.0 ± 0.1	0.297 ± 0.03	59.2±0.1	70.39± 0.2	12.10± 0.1
C15	124.1 ± 0.2	0.195 ± 0.02	58.4±0.1	71.94± 0.1	12.68± 0.1

All values are expressed as mean± SD (n=3); PDI: Polydispersity index; EE: Entrapment efficiency; DL: Drug loading

3.7.4. Scanning electron microscopy

The SEM image reveals the flaky structure of RFM whereas the SEM analysis of the RFM loaded nanoparticles revealed their spherical shape. The SEM results confirming the spherical shape of RFM nanoparticles suggest that there were hardly any flaky structure seen when RFM was loaded onto chitosan nanoparticles (Figure 6a-6b).

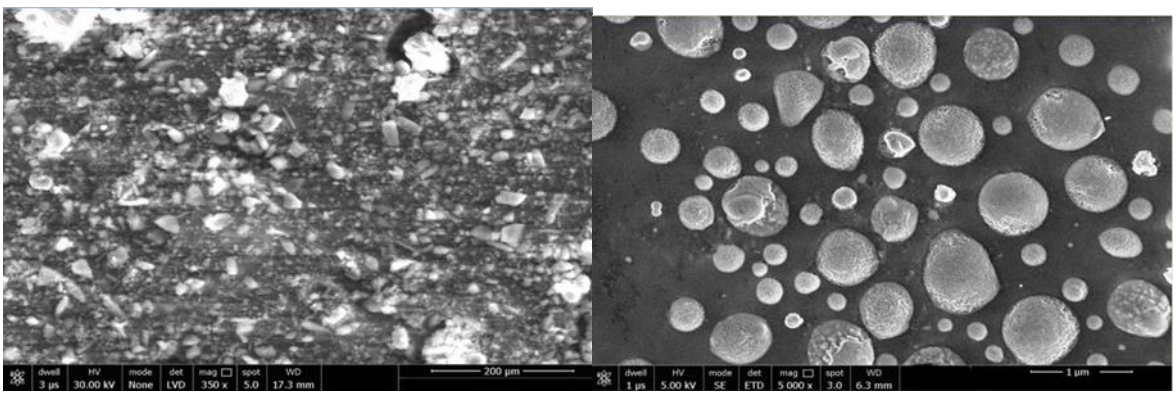

Figure 6a-6b SEM image of pure RFM and optimized formulation of batch C15

3.8. *In vitro* drug release

In vitro release study showed 100% release of pure RFM within 12 hrs (Figure 7). However, optimized chitosan nanoparticle formulation loaded with RFM showed nearly 90% release of RFM within 24 hr. The drug release from the nanoparticle system was found to follow the first order release kinetics (R2 = 0.9943) with the least sum of squared residual value. These results indicate that formulated nanoparticles prevent spreading of RFM over lung fluid before

they are taken up by alveolar macrophages. Therefore, in vitro results are implicated for greater exposure of maximum quantity of RFM to alveolar macrophages.

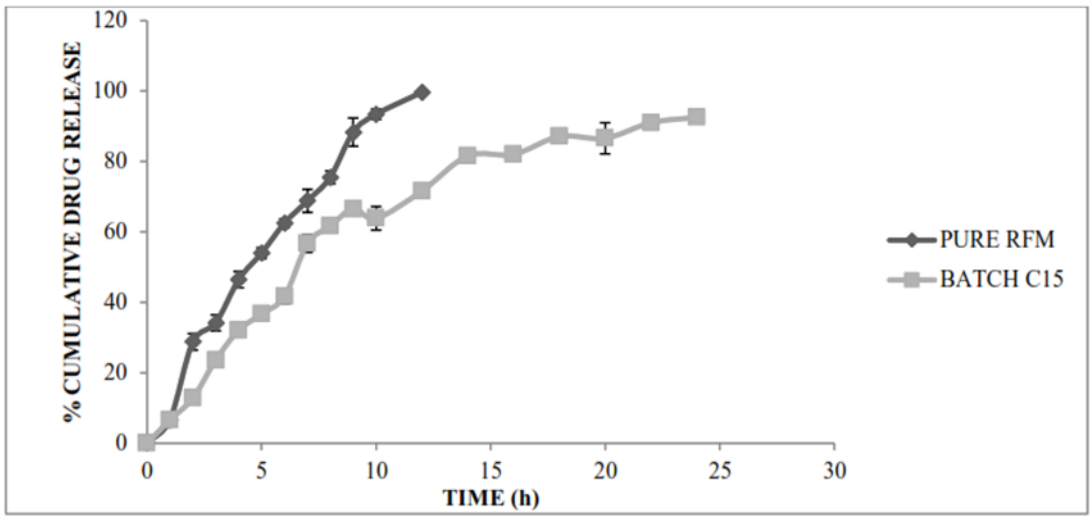

Figure 7 *In vitro* release studies of the optimized batch C15

4. Conclusion

The rifampicin loaded nanoparticle dry powder inhaler prepared using simple method exhibit uniform nanoparticle diameter, good dispersion, high drug loading and entrapment efficiency. The linearity of RFM was found within the concentration range of 10-75 µg/mL and the compatibility studies of rifampicin proved that the peaks and the functional groups of RFM were also present in the mixture of RFM with the lactose, chitosan, TPP as can be seen in the overlay spectra of RFM and its mixture with lactose. The 3- factor 3-level box behnken design was used to optimize nanoparticle formulation and achieved the response of optimum particle size, maximize entrapment efficiency and drug loading. This provides the basic conditions for invitro sustained release of small diameter particles, laying foundation for further study of pharmacokinetic data and targeted treatment in experimental animals with tuberculosis.

Compliance with ethical standards

Disclosure of conflict of interest

No conflict of interest to be disclosed.

References

[1] Smith I. Mycobacterium tuberculosis pathogenesis and molecular determinants of virulence. Clin Microbiol Rev. 2003 Jul;16(3):463-96.

[2] Aldovini, A., R. N. Husson, and R. A. Young. The uraA locus and homologous recombination in Mycobacterium bovis BCG. J. Bacteriol. 1993, 175: 7282-7289.

[3] Guidance for national tuberculosis programmes on the management of tuberculosis in children. Geneva: World Health Organization; 2006.

[4] Abate G, Hoffner SE. Synergistic antimycobacterial activity between ethambutol and the beta-lactam drug cefepime. Diagn Micr Infec Dis 1997;28:119–22.

[5] Llor C, Bjerrum L. Antimicrobial resistance: risk associated with antibiotic overuse and initiatives to reduce the problem. Ther Adv Drug Saf. 2014 Dec;5(6):229-41.

[6] Jin X, Song L, Ma CC, Zhang YC, Yu S. Pulmonary route of administration is instrumental in developing therapeutic interventions against respiratory diseases. Saudi Pharm J. 2020 Dec;28(12):1655-1665.

[7] Bruno BJ, Miller GD, Lim CS. Basics and recent advances in peptide and protein drug delivery. Ther Deliv. 2013 Nov;4(11):1443-67.

[8] Labiris NR, Dolovich MB. Pulmonary drug delivery. Part I: physiological factors affecting therapeutic effectiveness of aerosolized medications. Br J Clin Pharmacol. 2003 Dec;56(6):588-99.

[9] Ibrahim M, Verma R, Garcia-Contreras L. Inhalation drug delivery devices: technology update. Med Devices (Auckl). 2015 Feb 12;8:131-9.

[10] Rasul RM, Tamilarasi Muniandy M, Zakaria Z, Shah K, Chee CF, Dabbagh A, Rahman NA, Wong TW. A review on chitosan and its development as pulmonary particulate anti-infective and anti-cancer drug carriers. Carbohydr Polym. 2020 Dec 15;250:116800.

[11] Guo Y, Bera H, Shi C, Zhang L, Cun D, Yang M. Pharmaceutical strategies to extend pulmonary exposure of inhaled medicines. Acta Pharm Sin B. 2021 Aug;11(8):2565-2584.

[12] Gill P, Moghadam TT, Ranjbar B. Differential scanning calorimetry techniques: applications in biology and nanoscience. J Biomol Tech. 2010 Dec;21(4):167-93.

[13] Jain S, Shah RP. Drug-Excipient Compatibility Study Through a Novel Vial-in-Vial Experimental Setup: A Benchmark Study. AAPS PharmSciTech. 2023 May 10;24(5):117.

[14] Mikušová V, Mikuš P. Advances in Chitosan-Based Nanoparticles for Drug Delivery. Int J Mol Sci. 2021 Sep 6;22(17):9652.

[15] TIRUWA, R. A review on nanoparticles – preparation and evaluation parameters. Indian Journal of Pharmaceutical and Biological Research, 2016, 4(2), 27-31.

[16] Weng J, Tong HHY, Chow SF. In Vitro Release Study of the Polymeric Drug Nanoparticles: Development and Validation of a Novel Method. Pharmaceutics. 2020 Aug 4;12(8):732.